

Dissecting Galaxies with Quantitative Spectroscopy of the Brightest Stars in the Universe - Karl Schwarzschild Lecture 2009

Rolf-Peter Kudritzki^{1,*}

Institute for Astronomy, University of Hawaii, 2680 Woodlawn Dr., Honolulu, Hawaii 96822, USA

Received 30 December 2009, accepted 10 January 2010

Published online later

Key words galaxies: distances, galaxies: abundances, stars: early-type, stars: abundances, stars: distances

Measuring distances to galaxies, determining their chemical composition, investigating the nature of their stellar populations and the absorbing properties of their interstellar medium are fundamental activities in modern extragalactic astronomy helping to understand the evolution of galaxies and the expanding universe. The optically brightest stars in the universe, blue supergiants of spectral A and B, are unique tools for these purposes. With absolute visual magnitudes up to $M_V \cong -9.5$ they are the ideal to obtain accurate quantitative information about galaxies through the powerful modern methods of quantitative stellar spectroscopy. The spectral analysis of individual blue supergiant targets provides invaluable information about chemical abundances and abundance gradients, which is more comprehensive than the one obtained from H II regions, as it includes additional atomic species, and which is also more accurate, since it avoids the systematic uncertainties inherent in the strong line studies usually applied to the H II regions of spiral galaxies beyond the Local Group. Simultaneously, the spectral analysis yields stellar parameters and interstellar extinction for each individual supergiant target, which provides an alternative very accurate way to determine extragalactic distances through a newly developed method, called the Flux-weighted Gravity - Luminosity Relationship (FGLR). With the present generation of 10m-class telescopes these spectroscopic studies can reach out to distances of 10 Mpc. The new generation of 30m-class will allow to extend this work out to 30 Mpc, a substantial volume of the local universe.

© 2010 WILEY-VCH Verlag GmbH & Co. KGaA, Weinheim

1 Introduction

To measure distances to galaxies, to determine their chemical composition, and to investigate the nature of their stellar populations and the absorbing properties of their interstellar medium are fundamental activities in modern extragalactic astronomy. They are crucial to understand the evolution of galaxies and of the expanding universe and to constrain the history of cosmic chemical enrichment, from the metal-free universe to the present-day chemically diversified structure. However, while stars are the major constituents of galaxies, little of this activity is based on the quantitative spectroscopy of individual stars, a technique which over the last fifty years has proven to be one of the most accurate diagnostic tools in modern astrophysics. Given the distances to galaxies beyond the Local Group individual stars seem to be too faint for quantitative spectroscopy and, thus, astronomers have settled to restrict themselves to the photometric investigation of resolved stellar populations, the population synthesis spectroscopy of integrated stellar populations or the investigation of H II region-emission lines. Of course, color-magnitude diagrams and the study of nebular emission lines have an impressive diagnostic power, but they are also limited in many ways and subject to substantial systematic uncertainties, as we will show later in the course of this lecture.

Thus, is it really out of the question to apply the methods of quantitative spectroscopy of individual stars as a most powerful complementary tool to understand the evolution of galaxies beyond the Local Group? The answer is, no, it is not. In the era of 10m-class telescopes with most efficient spectrographs it is indeed possible to quantitatively analyze the spectra of individual stars in galaxies as distant as 10 Mpc and to obtain invaluable information about chemical composition and composition gradients, interstellar extinction and extinction laws as well as accurate extragalactic distances. With the even larger and more powerful next generation of telescopes such as the TMT and the E-ELT we will be able to extend such studies out to distances as large as 30 Mpc. All one has to do is to choose the right type of stellar objects and to apply the extremely powerful tools of NLTE spectral diagnostics, which have already been successfully tested with high resolution, high signal-to-noise spectra of similar objects in the Milky Way and the Magellanic Clouds.

Of course, now when studying objects beyond the Local Group the analysis methods need to be modified towards medium resolution spectra with somewhat reduced signal. For a stellar spectroscopist, who is usually trained to believe that only the highest resolution can give you an important answer, this requires some courage and boldness (or maybe naive optimism). But as we will see in the course of this lecture, once one has done this step, a whole new universe is opening up in the true sense of the word.

* Corresponding author: e-mail: kud@ifa.hawaii.edu

2 Choosing the Right Objects - A and B Supergiants

It has long been the dream of stellar astronomers to study individual stellar objects in distant galaxies to obtain detailed spectroscopic information about the star formation history and chemodynamical evolution of galaxies and to determine accurate distances based on the determination of stellar parameters and interstellar reddening and extinction. At the first glance, one might think that the most massive and, therefore, most luminous stars with masses higher than $50 M_{\odot}$ are ideal for this purpose. However, because of their very strong stellar winds and mass-loss these objects keep very hot atmospheric temperatures throughout their life and, thus, waste most of their precious photons in the extreme ultraviolet. As we all know, most of these UV photons are killed by dust absorption in the star forming regions, where these stars are born, and the few which make it to the earth can only be observed with tiny UV telescopes in space such as the HST or FUSE and are not accessible to the giant telescopes on the ground.

Thus, one learns quickly that the most promising objects for such studies are massive stars in a mass range between 15 to $40 M_{\odot}$ in the short-lived evolutionary phase, when they leave the hydrogen main-sequence and cross the HRD in a few thousand to ten thousand years as blue supergiants of B and early A spectral type. Because of the strongly reduced absolute value of bolometric correction when evolving towards smaller temperature these objects increase their brightness in visual light and become the optically brightest “normal” stars in the universe with absolute visual magnitudes up to $M_V \cong -9.5$ rivaling with the integrated light brightness of globular clusters and dwarf spheroidal galaxies. These are the ideal stellar objects to obtain accurate quantitative information about galaxies.

The optical spectra of B- and A-type supergiants are rich in metal absorption lines from several elements (C, N, O, Mg, Al, S, Si, Ti, Fe, among others). As young objects they represent probes of the current composition of the interstellar medium. Abundance determinations of these objects can therefore be used to trace the present abundance patterns in galaxies, with the ultimate goal of recovering their chemical and dynamical evolution history. In addition to the α -elements, key for a comparison with H II region results and to understand the chemical evolutionary status of each individual star, the stellar analysis of blue supergiants provides the only accurate way to obtain information about the spatial distribution of Fe-group element abundances in external star-forming galaxies. So far, beyond the Local Group most of the information about the chemical properties of spiral galaxies has been obtained through the study of H II regions oxygen emission lines using so-called strong-line methods, which, as we will show, have huge systematic uncertainties arising from their calibrations. Direct stellar abundance studies of blue supergiants open a completely new and more

accurate way to investigate the chemical evolution of galaxies.

In addition, because of their enormous intrinsic brightness, blue supergiants are also ideal distance indicators. As first demonstrated by Kudritzki, Bresolin & Przybilla (2003) there is a very simple and compelling way to use them for distance determinations. Massive stars with masses in the range from $12 M_{\odot}$ to $40 M_{\odot}$ evolve through the B and A supergiant stage at roughly constant luminosity. In addition, since the evolutionary timescale is very short when crossing through the B and A supergiant domain, the amount of mass lost in this stage is small. As a consequence, the evolution proceeds at constant mass and constant luminosity. This has a very simple, but very important consequence for the relationship between gravity and effective temperature along each evolutionary track, namely that the flux-weighted gravity, $g_F = g/T_{\text{eff}}^4$, stays constant. As shown in detail by Kudritzki, Urbaneja, Bresolin et al. (2008) and explained again further below this immediately leads to the ‘flux-weighted gravity–luminosity relationship’ (FGLR), which has most recently proven to be an extremely powerful to determine extragalactic distances with an accuracy rivalling the Cepheid- and the TRGB-method.

3 Spectral Diagnostics and Studies in the Milky Way and Local Group

The quantitative analysis of the spectra of these objects is not trivial. Most importantly, NLTE effects and but also the influence of stellar winds and atmospheric geometrical extension are of crucial importance. However, over the past decades with an effort of hundreds of men-years sophisticated model atmosphere codes for massive stars have been developed including the hydrodynamics of stellar winds and the accurate NLTE opacities of millions of spectral lines. Detailed tests have been carried out reproducing the observed spectra of Milky Way stars from the UV to the IR and constraining stellar parameters with unprecedented accuracy (see reviews by Kudritzki(1998), Kudritzki & Puls, 2000, Kudritzki & Urbaneja, 2009). For instance, the most recent work on A-type supergiants (Przybilla et al. 2006, 2008, Schiller & Przybilla (2008), see also Przybilla et al. (2000), Przybilla et al. (2001a), Przybilla et al. (2001b), Przybilla & Butler (2001), Przybilla (2002)) demonstrates that with high resolution and very high signal-to-noise spectra stellar parameters and chemical abundances can be determined with hitherto unknown precision (T_{eff} to $\leq 2\%$, $\log g$ to ~ 0.05 dex, individual metal abundances to ~ 0.05 dex).

At the same time, utilizing the power of the new 8m to 10m class telescopes, high resolution studies of A supergiants in many Local Group galaxies were carried out by Venn (1999) (SMC), McCarthy et al.(1995) (M33), McCarthy et al. (1997) (M31), Venn et al. (2000) (M31), Venn et al. (2001) (NGC 6822), Venn et al. (2003) (WLM),

and Kaufer et al. (2004) (Sextans A) yielding invaluable information about the stellar chemical composition in these galaxies. In the research field of massive stars, these studies have so far provided the most accurate and most comprehensive information about chemical composition and have been used to constrain stellar evolution and the chemical evolution of their host galaxies.

4 The Challenging Step beyond the Local Group

The concept to go beyond the Local Group and to study A supergiants by means of quantitative spectroscopy in galaxies out to the Virgo cluster has been first presented by Kudritzki, Lennon & Puls (1995) and Kudritzki (1998). Following-up on this idea, Bresolin, Kudritzki & Méndez et al. (2001) and Bresolin, Gieren & Kudritzki et al. (2002) used the VLT and FORS at 5 Å resolution for a first investigation of blue supergiants in NGC 3621 (6.7 Mpc) and NGC 300 (1.9 Mpc). They were able to demonstrate that for these distances and at this resolution spectra of sufficient S/N can be obtained allowing for the quantitative determination of stellar parameters and metallicities. Kudritzki, Bresolin & Przybilla (2003) extended this work and showed that stellar gravities and temperatures determined from the spectral analysis can be used to determine distances to galaxies by using the correlation between absolute bolometric magnitude and flux weighted gravity $g_F = g/T_{\text{eff}}^4$ (FGLR). However, while these were encouraging steps towards the use of A supergiants as quantitative diagnostic tools of galaxies beyond the Local Group, the work presented in these papers had still a fundamental deficiency. At the low resolution of 5 Å it is not possible to use ionization equilibria for the determination of T_{eff} in the same way as in the high resolution work mentioned in the previous paragraph. Instead, spectral types were determined and a simple spectral type - temperature relationship as obtained for the Milky Way was used to determine effective temperatures and then gravities and metallicities. Since the spectral type - T_{eff} relationship must depend on metallicity (and also gravities), the method becomes inconsistent as soon as the metallicity is significantly different from solar (or the gravities are larger than for luminosity class Ia) and may lead to inaccurate stellar parameters. As shown by Evans & Howarth (2003), the uncertainties introduced in this way could be significant and would make it impossible to use the FGLR for distance determinations. In addition, the metallicities derived might be unreliable. This posed a serious problem for the the low resolution study of A supergiants in distant galaxies.

This problem was overcome only very recently by Kudritzki, Urbaneja, Bresolin et al. (2008) (hereafter KUBGP), who provided the first self-consistent determination of stellar parameters and metallicities for A supergiants in galaxies beyond the Local Group based on the detailed

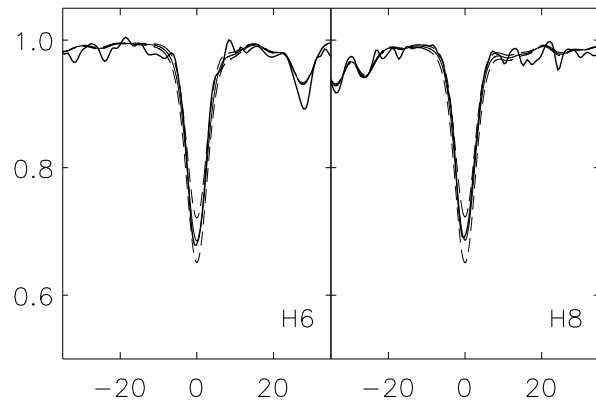


Fig. 1 Model atmosphere fit of two observed Balmer lines of NGC300 target No. 21 of KUBGP for $T_{\text{eff}} = 10000$ K and $\log g = 1.55$ (solid). Two additional models with same T_{eff} but $\log g = 1.45$ and 1.65, respectively, are also shown (dashed).

quantitative model atmosphere analysis of low resolution spectra. They applied their new method on 24 supergiants of spectral type B8 to A5 in the Sculptor Group spiral galaxy NGC 300 (at 1.9 Mpc distance) and obtained temperatures, gravities, metallicities, radii, luminosities and masses. The spectroscopic observations were obtained with FORS1 at the ESO VLT in multiobject spectroscopy mode. In addition, ESO/MPI 2.2m WFI and HST/ACS photometry was used. The observations were carried out within the framework of the Araucaria Project (Gieren et al. (2005b)). In the following we discuss the analysis method and the results of this pilot study.

5 A Pilot Study in NGC300 - The Analysis Method

For the quantitative analysis of the spectra KUBGP use the same combination of line blanketed model atmospheres and very detailed NLTE line formation calculations as Przybilla et al. (2006) in their high signal-to-noise and high spectral resolution study of galactic A-supergiants, which reproduce the observed normalized spectra and the spectral energy distribution, including the Balmer jump, extremely well. They calculate an extensive, comprehensive and dense grid of model atmospheres and NLTE line formation covering the potential full parameter range of all the objects in gravity ($\log g = 0.8$ to 2.5), effective temperature ($T_{\text{eff}} = 8300$ to 15000K) and metallicity ($[Z] = \log Z/Z_{\odot} = -1.30$ to 0.3). The total grid comprises more than 6000 models.

The analysis of the each of the 24 targets in NGC 300 proceeds in three steps. First, the stellar parameters (T_{eff} and $\log g$) are determined together with interstellar reddening and extinction, then the metallicity is determined and finally, assuming a distance to NGC 300, stellar radii, lumi-

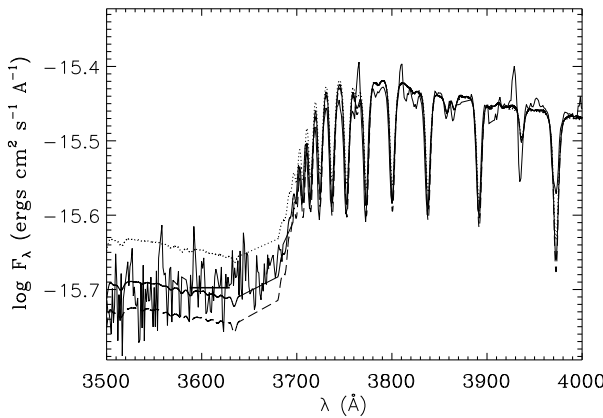


Fig. 2 Model atmosphere fit of the observed Balmer jump of the same target as in Fig. 1 for $T_{\text{eff}} = 10000$ K and $\log g = 1.55$ (solid). Two additional models with the same $\log g$ but $T_{\text{eff}} = 9750$ K (dashed) and 10500 K (dotted) are also shown. The horizontal bar at 3600 Å represents the average of the flux logarithm over this wavelength interval, which is used to measure D_B .

nosities and masses are obtained. For the first step, a well established method to obtain the stellar parameters of supergiants of late B to early A spectral type is to use ionization equilibria of weak metal lines (OI/II; MgI/II; NI/II etc.) for the determination of effective temperature T_{eff} and the Balmer lines for the gravities $\log g$. However, at the low resolution of 5 Å the weak spectral lines of the neutral species disappear in the noise of the spectra and an alternative technique is required to obtain temperature information. KUBGP confirm the result by Evans & Howarth (2003) that a simple application of a spectral type - effective temperature relationship does not work because of the degeneracy of such a relationship with metallicity. Fortunately, a way out of this dilemma is the use of the spectral energy distributions (SEDs) and here, in particular of the Balmer jump D_B . While the observed photometry from B-band to I-band is used to constrain the interstellar reddening, D_B turns out to be a reliable temperature diagnostic. A simultaneous fit of the Balmer lines and the Balmer jump allows to constrain effective temperature and gravity independent of assumptions on metallicity. Figure 1 and Fig. 2 demonstrate the sensitivity of the Balmer lines and the Balmer jump to gravity and effective temperature, respectively. The accuracy obtained by this method is $\leq 4\%$ for T_{eff} and ~ 0.05 dex for $\log g$.

Knowing the stellar atmospheric parameters T_{eff} and $\log g$ KUBGP are able to determine stellar metallicities by fitting the metal lines with their comprehensive grid of line formation calculations. The fit procedure proceeds again in several steps. First, spectral windows are defined, for which a good definition of the continuum is possible and which are relatively undisturbed by flaws in the spectrum (for in-

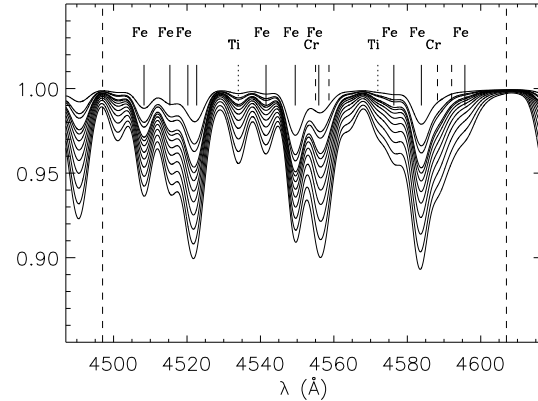


Fig. 3 Synthetic metal line spectra calculated for the stellar parameters of target No.21 as a function of metallicity in the spectral window from 4497 Å to 4607 Å. Metallicities range from $[Z] = -1.30$ to 0.30 , as described in the text. The dashed vertical lines give the edges of the spectral window as used for a determination of metallicity.

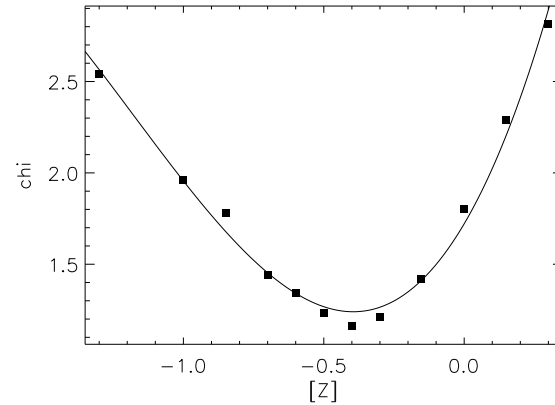


Fig. 5 $\chi([Z])$ as obtained from the comparison of observed and calculated spectra. The solid curve is a third order polynomial fit.

stance caused by cosmic events) or interstellar emission and absorption. A typical spectral window used for all targets is the wavelength interval 4497 Å $\leq \lambda \leq 4607$ Å. Figure 3 shows the synthetic spectrum calculated for the atmospheric parameters of the same target as analyzed in Fig. 1 and 2 for all the metallicities of the grid ranging from $-1.30 \leq [Z] \leq 0.30$. It is very obvious that the strengths of the metal line features are a strong function of metallicity.

In Fig. 4 the observed spectrum of the target in this spectral window is shown overplotted by the synthetic spectrum for each metallicity. Separate plots are used for each metallicity, because the optimal relative normalization of the observed and calculated spectra is obviously metallicity dependent. This problem is addressed by renormalizing the observed spectrum for each metallicity so that the synthetic spectrum always intersects the observations at the

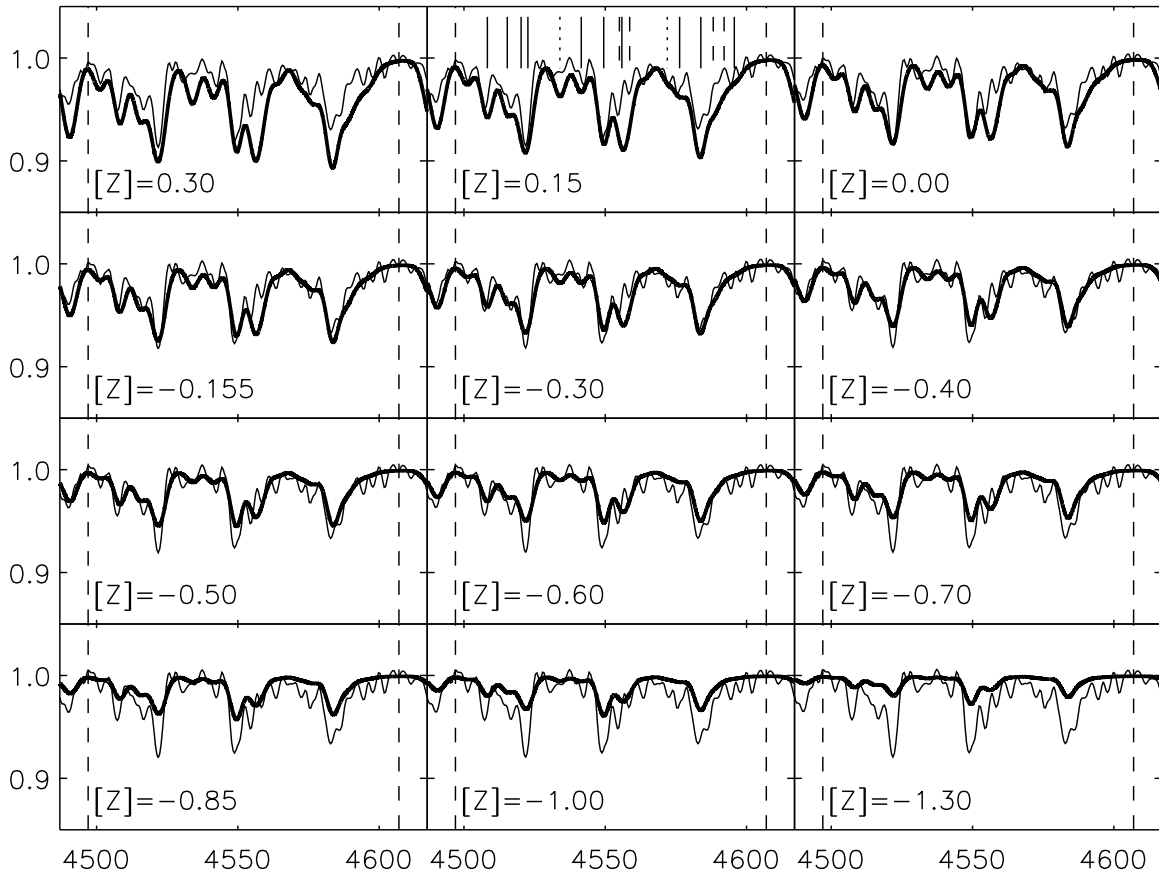


Fig. 4 Observed spectrum of the same target as in Fig. 1 and 2 in the same spectral window as Fig. 3 but now the synthetic spectra for each metallicity overplotted separately.

same value at the two edges of the spectral window (indicated by the dashed vertical lines). The next step is a pixel-by-pixel comparison of calculated and normalized observed fluxes for each metallicity and a calculation of a χ^2 -value. The minimum $\chi([Z])$ as a function of $[Z]$ is then used to determine the metallicity. This is shown in Fig. 5. Application of the same method on different spectral windows provides additional independent information on metallicity and allows to determine the average metallicity obtained from all windows. A value of $[Z] = -0.39$ is found with a very small dispersion of only 0.02 dex. However, one also need to consider the effects of the stellar parameter uncertainties on the metallicity determination. This is done by applying the same correlation method for $[Z]$ for models at the extremes of the error box for T_{eff} and $\log g$. This increases the uncertainty of $[Z]$ to ± 0.15 dex, still a very reasonable accuracy of the abundance determination.

After the determination of T_{eff} , $\log g$, and $[Z]$, the model atmosphere SED is used to determine interstellar reddening $E(B-V)$ and extinction $A_V = 3.1 E(B-V)$. Simultaneously, the fit also yields the stellar angular diameter, which provides the stellar radius, if a distance is adopted. Gieren et al. (2005a) in their multi-wavelength study of a

large sample of Cepheids in NGC 300 including the near-IR have determined a new distance modulus $m-M = 26.37$ mag, which corresponds to a distance of 1.88 Mpc. KUBGP have adopted these values to obtain the radii and absolute magnitudes.

6 A Pilot Study in NGC300 - Results

As a first result, the quantitative spectroscopic method yields interstellar reddening and extinction as a by-product of the analysis process. For objects embedded in the dusty disk of a star forming spiral galaxy one expects a wide range of interstellar reddening $E(B-V)$ and, indeed, a range from $E(B-V) = 0.07$ mag up to 0.24 mag was found (see Fig. 6). The individual reddening values are significantly larger than the value of 0.03 mag adopted in the HST distance scale key project study of Cepheids by Freedman et al. (2001) and demonstrate the need for a reliable reddening determination for stellar distance indicators, at least as long the study is restricted to optical wavelengths. The average over the observed sample is $\langle E(B-V) \rangle = 0.12$ mag in close agreement with the value of 0.1 mag found by Gieren et al. (2005a) in their optical to near-IR study of Cepheids in NGC 300.

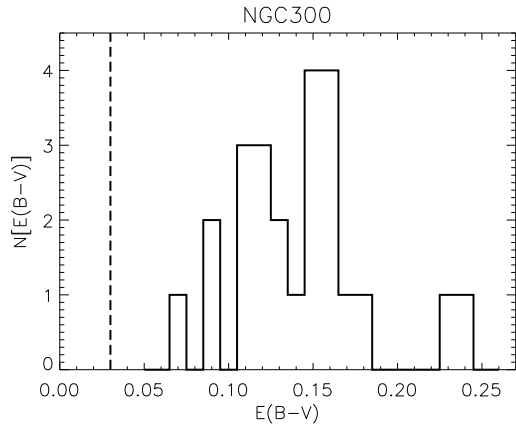


Fig. 6 Histogram of the reddening distribution of blue supergiants in NGC 300 determined from spectral analysis and photometry. The dashed lines show the $E(B-V)$ value adopted by the *HST* Key Project. Data from Kudritzki et al. (2008)

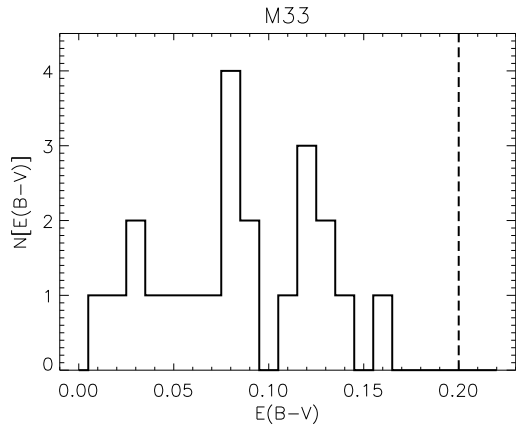


Fig. 7 Histograms of the reddening distribution of blue supergiants in M33. The dashed lines show the $E(B-V)$ value adopted by the *HST* Key Project. Data from U et al. (2009).

While Cepheids have somewhat lower masses than the A supergiants of our study and are consequently somewhat older, they nonetheless belong to the same population and are found at similar sites. Thus, one expects them to be affected by interstellar reddening in the same way as A supergiants.

Note that a difference of 0.1 mag in reddening corresponds to 0.3 mag in the distance modulus. It is, thus, not surprising that Gieren et al. (2005a) found a significantly shorter distance modulus for NGC 300 than the Key Project. Another illustrative example of the importance of an accurate determination of interstellar extinction is given in Fig. 7, which compares the reddening distribution obtained from the quantitative spectral analysis of blue supergiants in M33 with the value adopted by the Key Project. Again a

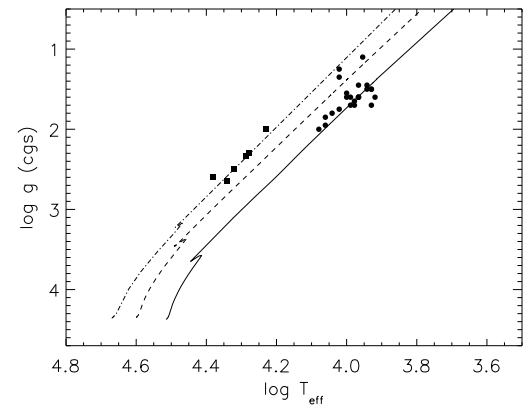


Fig. 8 NGC 300 A supergiants (filled circles) and early B supergiants (filled squares) in the $(\log g, \log T_{\text{eff}})$ plane compared with evolutionary tracks by Meynet & Maeder (2005) of stars with $15 M_{\odot}$ (solid), $25 M_{\odot}$ (dashed), and $40 M_{\odot}$ (dashed-dotted), respectively.

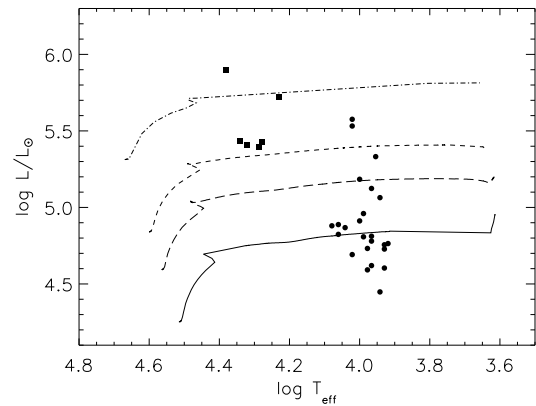


Fig. 9 NGC 300 A and early B supergiants in the HRD compared with evolutionary tracks for stars with $15 M_{\odot}$ (solid), $20 M_{\odot}$ (long-dashed), $25 M_{\odot}$ (short-dashed), and $40 M_{\odot}$ (dashed-dotted), respectively.

wide distribution in reddening is found, but this time the values are significantly smaller than the Key Project value (see discussion in section 9).

Figure 8 and Fig. 9 shows the location of all the observed targets in the $(\log g, \log T_{\text{eff}})$ plane and in the HRD. The diagrams include the early B-supergiants studied by Urbaneja et al. (2005b). The comparison with evolutionary tracks gives a first indication of the stellar masses in a range from $10 M_{\odot}$ to $40 M_{\odot}$. Three A supergiant targets have obviously higher masses than the rest of the sample and seem to be on a similar evolutionary track as the objects studied by Urbaneja et al. (2005b). The evolutionary information obtained from the two diagrams appears to be consistent. The B-supergiants seem to be more massive than most of the A supergiants. The same three A supergiants ap-

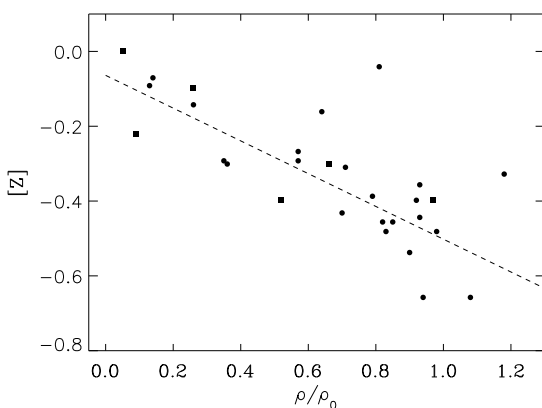


Fig. 10 Metallicity [Z] as a function of angular galactocentric distance ρ/ρ_0 for the A supergiants (filled circles) and early B-supergiants (filled squares). Note that for the latter metallicity refers to oxygen only. The dashed curve represents the regression discussed in the text.

parently more massive than the rest because of their lower gravities are also the most luminous objects. This confirms that quantitative spectroscopy is -at least qualitatively - capable to retrieve the information about absolute luminosities. Note that the fact that all the B supergiants studied by Urbaneja et al. (2005b) are more massive is simply a selection effect of the V magnitude limited spectroscopic survey by Bresolin, Gieren & Kudritzki et al. (2002). At similar V magnitude as the A supergiants those objects have higher bolometric corrections because of their higher effective temperatures and are, therefore, more luminous and massive.

Figure 10 shows the stellar metallicities and the metallicity gradient as a function of angular galactocentric distance, expressed in terms of the isophotal radius, ρ/ρ_0 (ρ_0 corresponds to 5.33 kpc). Despite the scatter caused by the metallicity uncertainties of the individual stars the metallicity gradient of the young disk population in NGC 300 is very clearly visible. A linear regression for the combined A- and B-supergiant sample yields (d in kpc, see also Bresolin et al. (2009b))

$$[Z] = -0.07 \pm 0.05 - (0.081 \pm 0.011) d. \quad (1)$$

Note that the metallicities of the B supergiants refer to oxygen only with a value of $\log N(O)/N(H) = -3.35$ adopted for the sun (Asplund et al. (2005)). On the other hand, the A supergiant metallicities reflect the abundances of a variety of heavy elements such as Ti, Fe, Cr, Si, S, and Mg. KUBGP discuss the few outliers in Fig. 10 and claim that these metallicities seem to be real. Their argument is that the expectation of homogeneous azimuthal metallicity in patchy star forming galaxies seems to be naive. Future work on other galaxies will show whether cases like this are common or not.

It is important to compare these results with metallicity measurements obtained from H II region emission lines. Be-

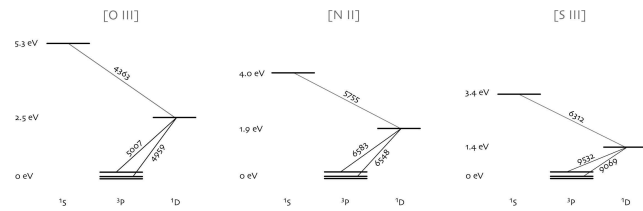


Fig. 11 Energy level diagrams for the strong and auroral nebular forbidden lines. The auroral lines arise from the higher excited levels. (Bresolin, priv. comm.)

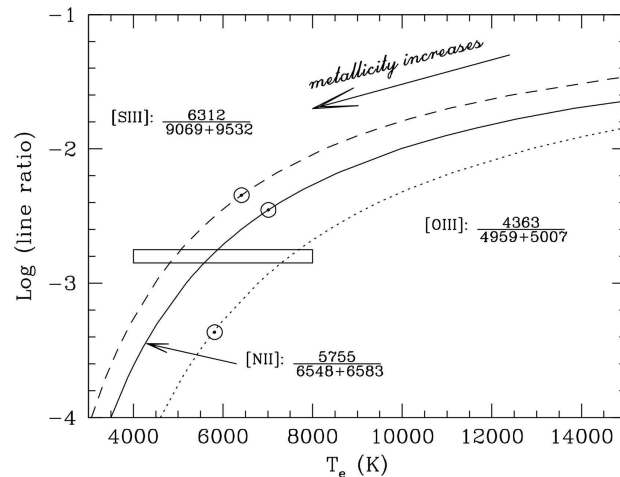


Fig. 12 Diagnostic of H II regions. Ratio of auroral to strong line fluxes as a function of nebular electron temperature. The horizontal box indicates the observational limit for 10m-class telescopes. (Bresolin, priv. comm.)

yond the Local Group and for metal rich galaxies H II region metallicities are mostly restricted to oxygen and measured through the so-called 'strong-line method', which uses the fluxes of the strongest forbidden lines of [O II] and [O III] relative to H β . Unfortunately, abundances obtained with the strong-line method depend heavily on the calibration used. Consequently, for the comparison of stellar with H II region metallicities KUBGP (extending the discussion started by Urbaneja et al. (2005b)) used line fluxes published by Deharveng et al. (1988) and applied various different published strong line method calibrations to determine nebular oxygen abundances, which could then be used to obtain the similar regressions as above.

As a very disturbing result, the different strong line method calibrations lead to significant differences in the central metallicity as well as in the abundance gradient. The calibrations by Dopita & Evans. (1986) and Zaritsky et al. (1994) predict a metallicity significantly supersolar in the center of NGC 300 contrary to the other calibrations. On the other hand, the work by KUBGP yields a central metallicity slightly smaller than solar in good agreement with Denicolo et al. (2002) and marginally agreeing with Kobulnicky et al. (1999), Pilyugin (2001), and Pettini & Pagel (2004). At the isophotal radius, 5.3 kpc

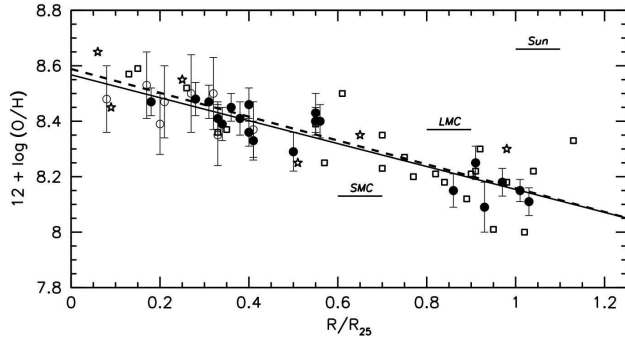


Fig. 13 Radial oxygen abundance gradient obtained from H II regions (circles) and blue supergiants (star symbols: B supergiants; open squares: A supergiants). The regression to the H II region data is shown by the continuous line. The dashed line represents the regression to the BA supergiant star data. For reference, the oxygen abundances of the Magellanic Clouds (LMC, SMC) and the solar photosphere are marked. From Bresolin, Gieren & Kudritzki et al. (2009a).

away from the center of NGC 300, KUBGP obtain an average metallicity significantly smaller than solar $[Z] = -0.50$, close to the average metallicity in the SMC. The calibrations by Dopita & Evans. (1986), Zaritsky et al. (1994), Kobulnicky et al. (1999) do not reach these small values for oxygen in the HII regions either because their central metallicity values are too high or the metallicity are gradients too shallow.

Thus, which of the metallicities determined for NGC 300 are correct? Those obtained from the blue supergiant study or the ones obtained from HII regions with one of the strong line calibrations? One possible way out of this problem is the use of the faint auroral emission lines (e.g. $[O\text{ III}]\lambda 4363$) of HII regions, instead of relying solely on strong lines, for nebular metallicity determinations (see Fig. 11). This requires a substantially larger observational effort at 10m-class telescopes. Bresolin, Gieren & Kudritzki et al. (2009a) have recently used FORS at the VLT and studied 28 HII regions in NGC 300, for all of which they were able to detect the auroral lines and to use them to constrain nebular electron temperatures (see Fig. 12). This allowed for a much more accurate determination of nebular oxygen abundances, avoiding the calibration uncertainty intrinsic to the strong-line method. The result of this work compared to the blue supergiant metallicities is shown in Fig. 13. The agreement between the stars and the HII regions is excellent, confirming independently the quality of the supergiant work and ruling out many of the strong line calibrations.

Bresolin, Gieren & Kudritzki et al. (2009a) also perform a very educative experiment. They use their new and very accurate measurements of strong line fluxes and simply apply a set of different more recent strong line calibrations to obtain oxygen abundances without using the information from the auroral lines. The result of this experiment com-

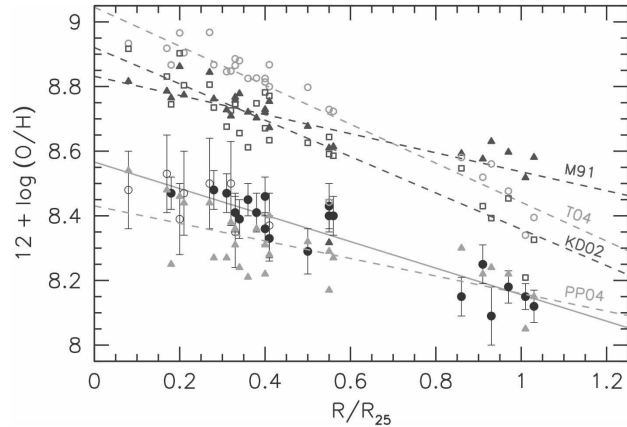


Fig. 14 H II region galactocentric oxygen abundance gradients in NGC 300 obtained from our dataset but different strong line calibrations: McGaugh 1991 = M91, Tremonti et al. 2004 = T04, Kewley & Dopita 2002 = KD02, and Pettini & Pagel 2004 = PP04, as shown by the labels to the corresponding least squares fits. The auroral line-based abundances determined by Bresolin et al. (2009a) are shown by the full and open circle symbols, and the corresponding linear fit is shown by the continuous line.

pared with the oxygen abundances using the auroral lines is shown in Fig. 14. The comparison is again shocking. The abundance offsets introduced by the application of inappropriate strong-line calibrations can be as large as 0.6 dex, putting the whole business of constraining galaxy evolution through the measurement of nebular metallicities and metallicity gradients into jeopardy.

7 The Metallicities of Galaxies

As is well known, the metallicity of the young stellar population of spiral galaxies has the potential to provide important constraints on galactic evolution and the chemical evolution history of the universe. For instance, the relationship between central metallicity and galactic mass appears to be a Rosetta stone to understand chemical evolution and galaxy formation (Lequeux et al. (1979), Tremonti et al. (2004), Maiolino et al. (2008)). In addition, the observed metallicity gradients in spiral galaxies, apparently large for spirals of lower mass and shallow for high mass galaxies (Garnett et al. (1997), Skillman (1998), Garnett (2004)), are the result of a complex interplay of star formation history, initial mass function and matter infall into the disks of spirals and allow in principle to trace the evolutionary history of spiral galaxies. However, as intriguing the observations of the mass-metallicity relationship and the metallicity gradients of galaxies are, the published results are highly uncertain in a quantitative sense, since they reflect the intrinsic uncertainty of the calibration of the strong line method applied. As a striking example, Kewley & Ellison (2008) have demonstrated that the quan-

Table 1 Central metallicity [Z] and metallicity gradient (dex/kpc) in NGC 300.

Source	Central Abundance	Gradient	Comments
Dopita & Evans(1986)	0.29±0.17	-0.118±0.019	HII, oxygen
Zaritsky et al. (1994)	0.32±0.04	-0.101±0.017	HII, oxygen
Kobulnicky et al. (1999)	0.09±0.04	-0.051±0.017	HII, oxygen
Denicolo et al. (2002)	-0.05±0.05	-0.086±0.019	HII, oxygen
Pilyugin (2001)	-0.14±0.06	-0.053±0.023	HII, oxygen
Pettini & Pagel (2004)	-0.16±0.04	-0.068±0.015	HII, oxygen
KUBGP	-0.07±0.09	-0.081±0.011	stars, metals

titative shape of the mass-metallicity relationship of galaxies can change from very steep to almost flat depending on the calibration used (Fig. 15). In the same way and as demonstrated by Fig. 14, and Tab. 1 metallicity gradients of spiral galaxies can change from steep to flat simply as the result of the calibration used. Obviously, the much larger effort of either stellar spectroscopy of blue supergiants or the observation of faint nebular auroral lines will be needed in the future to observationally constrain the metallicities and metallicity gradients of spiral galaxies and their evolutionary history. We note that the use of blue supergiants provides the additional information about chemical abundances of iron-group elements as an important additional constraint of galaxy evolution history.

8 Flux Weighted Gravity - Luminosity Relationship (FGLR)

Massive stars with masses in the range from $12 M_{\odot}$ to $40 M_{\odot}$ evolve through the B and A supergiant stage at roughly constant luminosity (see Fig. 5). In addition, since the evolutionary timescale is very short when crossing through the B and A supergiant domain, the amount of mass lost in this stage is small. This means that the evolution proceeds at constant mass and constant luminosity. This has a very simple, but very important consequence for the relationship of gravity and effective temperature along each evolutionary track. From

$$L \propto R^2 T_{\text{eff}}^4 = \text{const.}; M = \text{const.} \quad (2)$$

follows immediately that

$$M \propto g R^2 \propto L (g/T_{\text{eff}}^4) = L g_F = \text{const.} \quad (3)$$

Thus, along the evolution through the B and A supergiant domain the “flux-weighted gravity” $g_F = g/T_{\text{eff}}^4$ should remain constant. This means each evolutionary track of different luminosity in this domain is characterized by a specific value of g_F . This value is determined by the relationship between stellar mass and luminosity, which in a first approximation is a power law

$$L \propto M^x \quad (4)$$

and leads to a relationship between luminosity and flux-weighted gravity

$$L^{1-x} \propto (g/T_{\text{eff}}^4)^x. \quad (5)$$

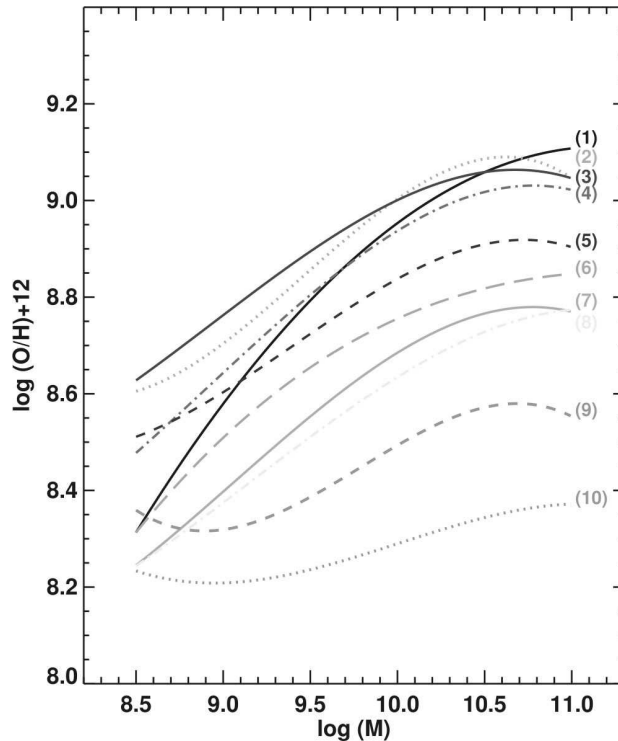


Fig. 15 The mass-metallicity relationship of star forming galaxies in the nearby universe obtained by applying several widely used empirical metallicity calibrations based on different strong line ratios. This figure illustrates that there is an effect not only on the absolute scale, but also on the relative shape of this relationship. Adapted from Kewley & Ellison (2008).

With the definition of bolometric magnitude $M_{\text{bol}} \propto -2.5 \log L$ one then derives

$$-M_{\text{bol}} = a_{\text{FGLR}}(\log g_F - 1.5) + b_{\text{FGLR}}. \quad (6)$$

This is the “flux-weighted gravity – luminosity relationship” (FGLR) of blue supergiants. Note that the proportionality constant a_{FGLR} is given by the exponent of the mass – luminosity power law through

$$a_{\text{FGLR}} = 2.5x/(1-x), \quad (7)$$

for instance, for $x = 3$, one obtains $a_{\text{FGLR}} = -3.75$. Note that the zero point of the relationship is chosen at a flux weighted gravity of 1.5, which is in the middle of the range encountered for blue supergiant stars.

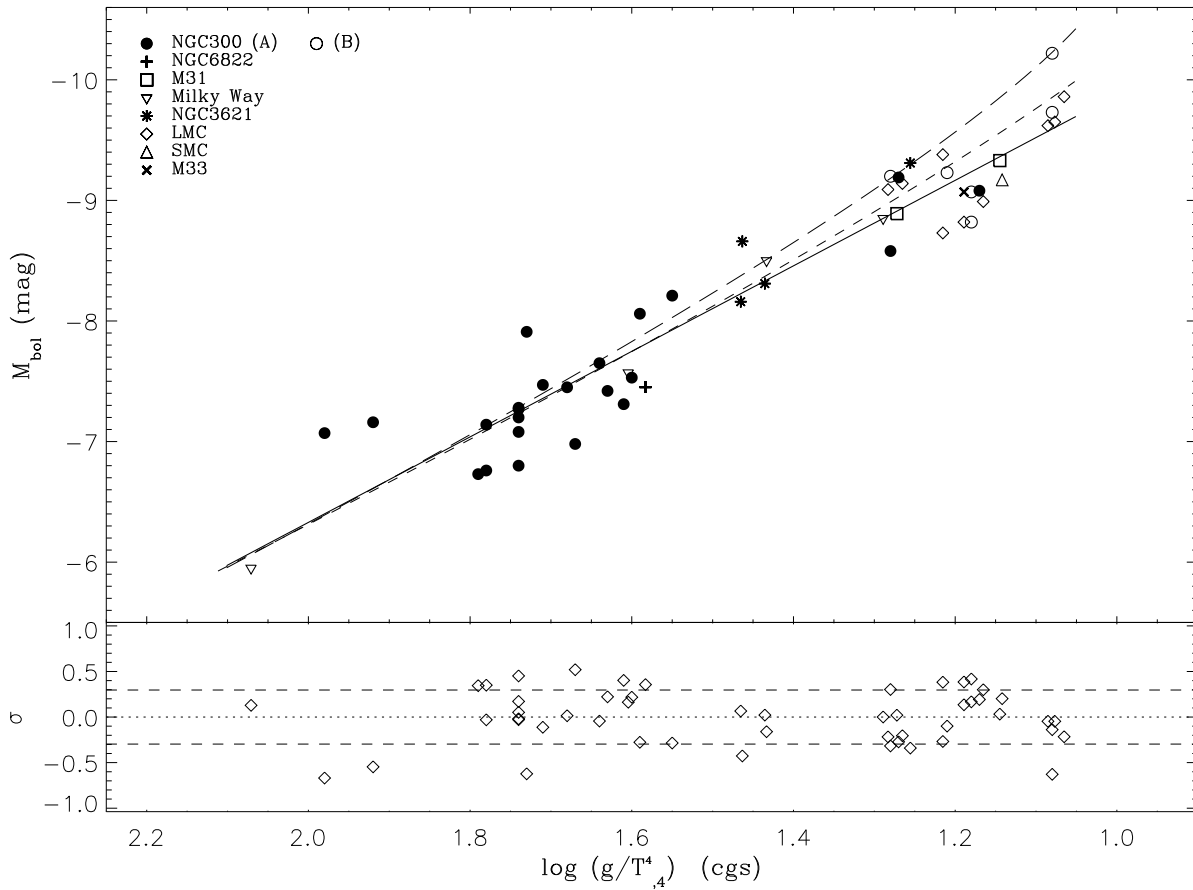


Fig. 17 The FGLR of A (solid circles) and B (open circles) supergiants in 8 galaxies including NGC 300 and the linear regression (solid). The stellar evolution FGLRs for models with rotation are again overplotted.

KUBGP use the mass-luminosity relationships of different evolutionary tracks (with and without rotation, for Milky Way and SMC metallicity) to calculate the FGLRs predicted by stellar evolution. Very interestingly, while different evolutionary model types yield somewhat different FGLRs, the differences are rather small.

Kudritzki, Bresolin & Przybilla (2003) were the first to realize that the FGLR has a very interesting potential as a purely spectroscopic distance indicator, as it relates two spectroscopically well defined quantities, effective temperature and gravity, to the absolute magnitude. Compiling a large data set of spectroscopic high resolution studies of A supergiants in the Local Group and with an approximate analysis of low resolution data of a few targets in galaxies beyond the Local Group (see discussion in previous chapters) they were able to prove the existence of an observational FGLR rather similar to the theoretically predicted one.

With the improved analysis technique of low resolution spectra of A supergiants and with the much larger sample studied for NGC 300 KUBGP resumed the investigation of the FGLR. The result is shown in Fig. 16, which for NGC 300 reveals a clear and rather tight relationship of flux

weighted gravity $\log g_F$ with bolometric magnitude M_{bol} . A simple linear regression yields $b_{FGLR} = 8.11$ for the zero point and $a_{FGLR} = -3.52$ for the slope. The standard deviation from this relationship is $\sigma = 0.34$ mag. Within the uncertainties the observed FGLR appears to be in agreement with the theory.

In their first investigation of the empirical FGLR Kudritzki, Bresolin & Przybilla (2003) have added A supergiants from six Local Group galaxies with stellar parameters obtained from quantitative studies of high resolution spectra (Milky Way, LMC, SMC, M31, M33, NGC 6822) to their results for NGC 300 to obtain a larger sample. They also added 4 objects from the spiral galaxy NGC 3621 (at 6.7 Mpc) which were studied at low resolution. KUBGP added exactly the same data set to their new enlarged NGC 300 sample, however, with a few minor modifications. For the Milky Way they included the latest results from Przybilla et al. (2006) and Schiller & Przybilla (2008) and for the two objects in M31 we use the new stellar parameters obtained by Przybilla et al. (2008a). For the objects in NGC 3621 they applied new HST photometry. They also re-analyzed the LMC objects using ionization equilibria for the temperature determination.

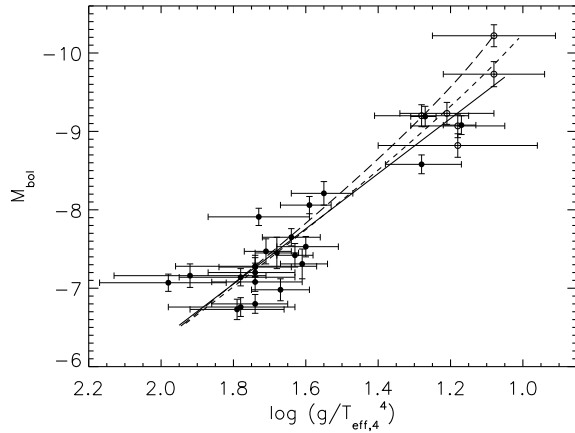


Fig. 16 The FGLR of A (solid circles) and B (open circles) supergiants in NGC 300 and the linear regression (solid). The stellar evolution FGLRs for models with rotation are also overplotted (dashed: Milky Way metallicity, long-dashed: SMC metallicity).

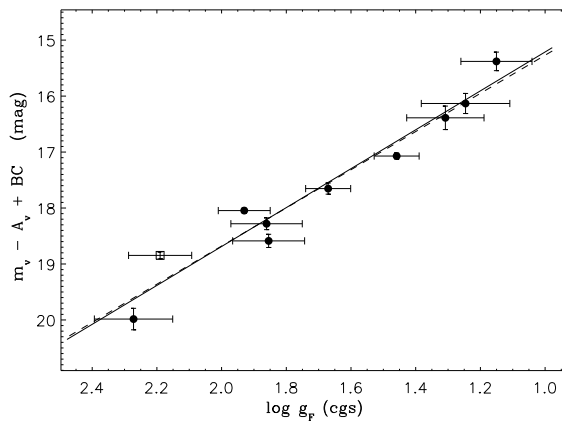


Fig. 18 The FGLR of the Local Group dwarf irregular galaxy WLM, based on apparent bolometric magnitudes ($m_{bol} = m_v - A_v + BC$). The solid line corresponds to the FGLR calibration. The distance is determined by using this calibration through a minimization of the residuals. From Urbaneja, Kudritzki & Bresolin et al. 2008.

Fig. 17 shows bolometric magnitudes and flux-weighted gravities for the full sample of eight galaxies again revealing a tight relationship over one order of magnitude in flux-weighted gravity. The linear regression coefficients are $a_{FGLR} = -3.41 \pm 0.16$ and $b_{FGLR} = 8.02 \pm 0.04$, very similar to the NGC 300 sample alone. The standard deviation is $\sigma = 0.32$ mag. The stellar evolution FGLR for Milky Way metallicity provides a fit of almost similar quality with a standard deviation of $\sigma = 0.31$ mag.

9 First Distances Using the FGLR-Method

With a relatively small residual scatter of $\sigma \sim 0.3$ mag the observed FGLR with the calibrated values of a_{FGLR}

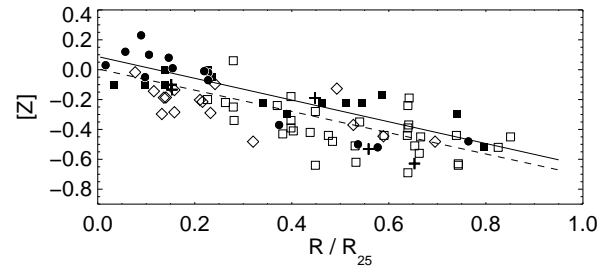


Fig. 19 Metallicity of blue supergiants, H II regions and Cepheids as a function of dimensionless angular galactocentric distance in the triangulum galaxy M33. A supergiants (circles) and B supergiants (squares) are shown as solid symbols. Logarithmic oxygen abundances of H II regions in units of the solar value as published by Magrini et al. (2007) are plotted as open squares. Logarithmic neon abundances of H II regions normalized to the value for B stars in the solar neighbourhood and as obtained from Rubin et al. (2008) are shown as large open diamonds. The metallicity [Z] for beat Cepheids as determined by Beaulieu et al. (2006) are given as crosses. The solid line is the regression for the supergiants only, whereas the dashed lines is the regression for all objects.

and b_{FGLR} is an excellent tool to determine accurate spectroscopic distance to galaxies. It requires multicolor photometry and low resolution (5 Å) spectroscopy to determine effective temperature and gravity and, thus, flux-weighed gravity directly from the spectrum. With effective temperature, gravity and metallicity determined one also knows the bolometric correction, which is particularly small for A supergiants. This means that errors in the stellar parameters do not largely affect the determination of bolometric magnitudes. Moreover, one knows the intrinsic stellar SED and, therefore, can determine interstellar reddening and extinction from the multicolor photometry, which then allows for the accurate determination of the reddening-free apparent bolometric magnitude. The application of the FGLR then yields absolute magnitudes and, thus, the distance modulus.

The first distance determination of this type has been carried out by Urbaneja, Kudritzki & Bresolin et al. 2008 who studied blue supergiants in WLM, one of faintest dwarf irregular galaxies in the Local Group. The quantitative spectral analysis of VLT FORS spectra yields an extremely low metallicity of the young stellar population in this galaxy with an average of -0.9 dex below the solar value. The interstellar extinction is again extremely patchy ranging from 0.03 to 0.30 mag in E(B-V) (note that the foreground value given by Schlegel et al. (1998) is 0.037 mag). The individually de-reddened FGLR - in apparent bolometric magnitude - is shown in Fig. 18. Using the FGLR calibration by Kudritzki, Urbaneja, Bresolin et al. (2008) and minimizing the residuals Urbaneja, Kudritzki & Bresolin et al. 2008 determined a distance modulus of 24.99 ± 0.10 mag (995 ± 46

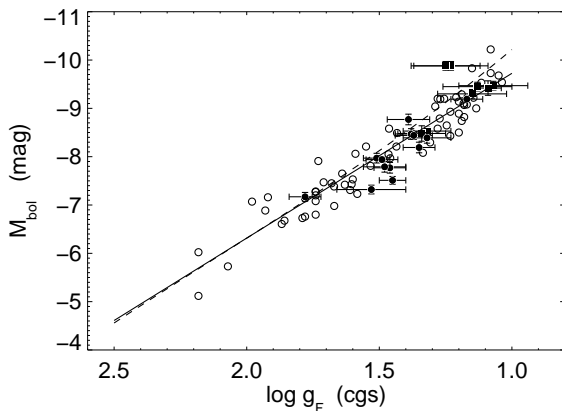


Fig. 20 FGLR fits of the blue supergiants in M33. Solid circles are late B and A supergiants and solid squares are early B supergiants in M33. The solid line is a linear fit as described in the text. In addition to the M33 targets, objects from nine other galaxies investigated in the studies by K08 and Urbaneja, Kudritzki & Bresolin et al. 2008 are also shown. The solid line is the regression FGLR from K08. The dashed curve is the stellar evolution FGLR for Milky Way metallicity.

kpc). This value is in good agreement with the TRGB distance by Rizzi et al. 2007 and the K-band Cepheid distance by Gieren et al. (2008), albeit 0.07 mag larger.

Most recently, U, Urbaneja & Kudritzki et al. 2009 have analyzed blue supergiant spectra obtained with DEIMOS and ESI at the Keck telescopes to determine a distance to the triangulum galaxy M33. The case of M33 is particularly interesting, since many independent distance determinations have been carried out for this galaxy during the last decade using a variety of techniques, including Cepheids, RR Lyrae, TRGB, red clump stars, planetary nebulae, horizontal branch stars and long-period variables. The surprising result of all of these studies has been that the distance moduli obtained with these different methods differ by as much as 0.6 mag, which is more than 30% in the linear distance. At the same time, also the metallicity and the metallicity gradient of the young stellar population in the disk of M33 are still heavily disputed. Different published results obtained from H II region work range from no gradient at all (Rosolowsky & Simon (2008)) to a very steep gradient of -0.11 dex/kpc (Garnett et al. (1997)) and everywhere in between (Willner & Nelson-Patel (2002), Magrini et al. (2007)) including a bimodal break with a very steep inner gradient (Vilchez et al. (1988), Magrini et al. (2007)).

The blue supergiant spectroscopy by U, Urbaneja & Kudritzki et al. 2009 supports a moderate metallicity gradient of 0.07dex/kpc without any indication of a bimodal break (see Fig. 19). The FGLR-method (Fig. 20) yields a long distance modulus for M33 of 24.93 ± 0.11 mag, in basic agreement with a TRGB

distance of 24.84 ± 0.10 mag obtained by the same authors from HST ACS imaging. The long distance modulus agrees also very well with the eclipsing binary distance obtained by Bonanos, Stanek & Kudritzki et al. (2006). U, Urbaneja & Kudritzki et al. 2009 relate the difference between their result and the published cepheid distances to the difference in accounting for interstellar reddening (see Fig. 7).

These successfull first applications of the FGLR-method for distance determinations indicate the very promising potential of the method to provide an independent constraint on the extragalactic distance scale.

10 The Potential of FGLR-Method for extragalactic Distance Determinations

One of the most challenging chapters of modern astrophysics is the effort to establish the extragalactic distance scale with with sufficient accuracy. Over the past years, substantial improvement has been made by the *HST Key Project on the Extragalactic Distance Scale* (Freedman et al. (2001)) and by the *SN Ia HST Calibration Program* (Saha et al. (2001), Sandage et al. (2006)), in which Cepheid-based distances to galaxies permitted the calibration of far-reaching secondary indicators. In addition, the ‘Tip of the Red Giant Branch’ (TRGB) method has become an additional very reliable and effective extragalactic distance indicator (Rizzi et al. 2007), which can also be used to calibrate secondary indicators (Mould & Sakai, 2008, 2009ab). However, in spite of this progress, there are still a number of systematic uncertainties which affect both, the Cepheids and secondary methods of distance measurement, and which do not yet allow to obtain extragalactic distances, and thus the Hubble constant, with the high accuracy desired and needed by cosmologists, i.e. below the current 10% uncertainty. For instance, the results on the Hubble constant H_0 obtained by Freedman et al. (2001) and Sandage et al. (2006) differ by 20% and the agreement with the TRGB-based calibration and the HST Key Project is at the margin of 10%. As is well known (see the discussion in Macri et al. 2006, section 4.6), the determination of cosmological parameters from the cosmic microwave background is affected by degeneracies in parameter space and cannot provide strong constraints on the value of H_0 (Spergel (2006), Tegmark et al., (2004)). Only, if assumptions are made, for instance that the universe is flat, H_0 can be predicted with high precision (i.e. 2%) from the observations of the cosmic microwave background, baryonic acoustic oscillations and type I high redshift supernovae. If these assumptions are relaxed, then much larger uncertainties are introduced (Spergel et al. (2007), Komatsu et al. (2009)). As an example, the uncertainty of the determination of the dark energy equation-of-state parameter $w = p/(c\rho^2)$ is related to the uncertainty of the Hubble constant through $\delta w/w \sim 2\delta H_0/H_0$. Thus, an independent determination of H_0 with an accuracy of 5% will allow

to reduce the 1σ uncertainty of the cosmological equation of state parameter w to ± 0.1 . A combination with other independent measurements constraining the cosmological parameters (large scale structure, SN Ia) will then allow for even tighter constraints. A very promising step forward in this regard has been made most recently by Riess et al., (2009ab), but it is clear that the complexity of their approach requires additional and independent tests.

Among the remaining uncertainties affecting the extragalactic distance scale, probably the most important one is interstellar reddening. As young stars, Cepheids tend to be embedded in dusty regions which produce a significant *internal* extinction, in addition to the galactic foreground extinction. It seems likely that most of the Cepheid distances to galaxies determined from optical photometry *alone* are affected by sizeable systematic errors, due to a flawed determination of the appropriate reddening correction. The examples for NGC 300 and M33 give in the sections above clearly illustrate the problem. IR photometry (J, H and K-band) of Cepheids is a promising way to address the issue, as has been shown in the Araucaria collaboration (Gieren et al. (2005b)) or by Riess et al. (2009b). However, photometry at these wavelengths is still subject to important systematic effects, thus an entirely independent and complementary approach to address the issue of reddening is highly desirable.

The TRGB method is, in principle, not free from reddening errors, too. Usually, fields in the outskirts of the galaxies investigated are observed and Galactic foreground reddening values obtained from the interpolation of published maps are used to apply an extinction correction. While this seems to be a reasonable assumption, it has also been demonstrated that for a few galaxies (NGC 300, Vlajic et al. (2009); M83, Bresolin et al. (2009b)) the stellar disks extend much further out than previously assumed and what the intrinsic reddening is in these very faint extended disks is completely unexplored. In the application of the TRGB method, colors are used to constrain metallicity and cannot, therefore, provide information about reddening.

An equally important uncertainty in the use of Cepheids as distance indicators is the dependence of the period-luminosity (P-L) relationship on metallicity. Work by Kennicutt et al. (1998) on M101 and by Macri et al. (2006) on the maser galaxy NGC 4258 using metallicity gradient information from H II region oxygen emission lines (Cepheids beyond the Local Group are too faint for a determination of their metallicity directly from spectra) indicates an *increase of Cepheid brightness with metallicity*. This agrees with Sakai et al. (2004), who related the difference between TRGB and Cepheid distances to the galactic H II region metallicities (not taking into account metallicity gradients, though) and derived a similar P-L dependence on metallicity.

However, these results are highly uncertain. Rizzi et al. 2007 have argued that many of the TRGB distances used by Sakai et al. (2004) need to be revised. With

the Rizzi et al. 2007 TRGB distances the Sakai et al. (2004) dependence of the P-L relationship on metallicity disappears and the results are in much closer agreement with stellar pulsation theory (Fiorentino et al. (2002), Marconi et al. (2005), Bono et al. (2008)), which predicts a small *decrease of Cepheid brightness with metallicity*. Moreover, all the H II region (oxygen) metallicities adopted when comparing Cepheid distances with TRGB distances or when using metallicity gradients are highly uncertain. They result from the application of the “strong-line method”, using the calibration by Zaritsky et al. (1994). As we have shown above, this calibration gives metallicities and metallicity gradients that are not in agreement with results obtained from blue supergiants or from H II regions, when the more accurate method involving auroral lines is used. We point out, following the discussion in Macri et al. (2006), that even small changes in the P-L metallicity dependence can have an effect of several percent on the determination of H_0 . We also note that the , most recent work by Riess et al. (2009b) makes use of this calibration.

Also the TRGB method has a metallicity dependence. Usually, the metallicity of the old metal-poor population used for the method is obtained from the $V - I$ color, assuming that only foreground reddening is important. Then, a calibration of the TRGB magnitude as a function of metallicity is used. As shown in the careful work by Mager et al. (2008) on the TRGB distance to the maser galaxy NGC 4258, this metallicity correction introduces a systematic uncertainty of 0.12 mag in the distance modulus.

Very obviously, in order to improve the determination of extragalactic distances of star-forming spiral and irregular galaxies in the local universe an independent and complementary method is desirable, which can overcome the problems of interstellar extinction and variations of chemical composition. The FGLR-method presented in the two previous sections is such a method. The tremendous advantage of this technique is that individual reddening and extinction values, together with metallicity, can be determined for each supergiant target directly from spectroscopy combined with photometry. This reduces significantly the uncertainties affecting competing methods such as cepheids and the TRGB.

The FGLR technique is robust. Bresolin et al. 2004, 2006 have shown, from observations in NGC 300 and WLM, that the photometric variability of blue supergiants has negligible effect on the distances determined through the FGLR. Moreover, the study by Bresolin et al. (2005) also confirms that with *HST* photometry the FGLR method is not affected by crowding out to distances of at least 30 Mpc. This is the consequence of the enormous intrinsic brightness of these objects, which are 3 to 6 magnitudes brighter than Cepheids.

The current calibration of the FGLR rests on the 5 Å resolution stellar spectra obtained in NGC 300 and in seven additional galaxies (in some cases with higher resolution).

Ideally, a large number of stars, observed in a single galaxy with a well-established distance, should be used. Obviously, a very natural step to improve the precision of the method by recalibrating in the LMC. The LMC currently defines the zero point for many classic photometric distance indicators, and its distance is presently well constrained, e.g. from eclipsing binaries ($m - M = 18.50 \pm 0.06$, Pietrzynski et al. (2009)). This work is presently under way. In addition, the analysis of a large sample of SMC blue supergiants will provide additional information about the metallicity dependence of the method, but also about the geometrical depth of the SMC. New spectra in IC 1613 (10% solar metallicity) and M31 (\sim solar metallicity) will help to constrain how the FLRG depends on metallicity, even though the results already obtained on WLM (10% solar metallicity, Urbaneja, Kudritzki & Bresolin et al. 2008) does not indicate a strong effect.

An alternative and certainly more ambitious approach will be to by-pass the LMC as a distance scale anchor point and to use the maser galaxy NGC 4258 (Humphreys et al. (2008)) as the ultimate calibrator. While challenging, such a step would be entirely feasible and provide an independent test of the approach taken by Riess et al. (2009ab). Last but not least, the GAIA mission will provide a very accurate determination of the distances of blue supergiants in the Milky Way, which will allow for an accurate local calibration of the FLRG.

11 Perspectives of Future Work

It is evident that the type of work described in this paper can be in a straightforward way extended to the many spiral galaxies in the local volume at distances in the 4 to 12 Mpc range. Bresolin, Kudritzki & Méndez et al. (2001) have already studied A supergiants in NGC 3621 at a distance of 7 Mpc. Pushing the method we estimate that with present day 8m to 10m class telescopes and the existing very efficient multi-object spectrographs one can reach down with sufficient S/N to $V = 22.5$ mag in two nights of observing time under very good conditions. For objects brighter than $M_V = -8$ mag this means metallicities and distances can be determined out to distances of 12 Mpc ($m - M = 30.5$ mag). This opens up a substantial volume of the local universe for metallicity and galactic evolution studies and independent distance determinations complementary to the existing methods. With the next generation of extremely large telescopes such as the TMT, GMT or the E-ELT the limiting magnitude can be pushed to $V = 24.5$ equivalent to distances of 30 Mpc ($m - M = 32.5$ mag).

Acknowledgements. The work presented here is the result of an ongoing collaborative effort over many years. I wish to thank my colleagues in Hawaii Miguel Urbaneja, Fabio Bresolin and Vivian U for their tremendous dedication and skillful contributions to help me to make this project happen. It is more than just a science collaboration. It is a joyful endeavor with a lot of challenges but also a lot of fun. My colleagues Norbert Przybilla and Florian Schiller

from Bamberg Observatory have made crucial contributions without which this project would not have been possible. I hope that the good time we had together in Hawaii has been an adequate compensation for their efforts. I also want to thank Wolfgang Gieren and his team from Universidad de Concepcion for inviting us to be part of the Araucaria collaboration. This has given a much wider perspective to our project. It has also created the new spirit of a “trans-Pacific” collaboration.

References

Allende Prieto, C., Lambert, D.L., & Asplund, M. 2001, *ApJ*, 556, L63
 Asplund, M., Grevesse, N., Sauval, A.J., 2005, ASP Conf. Series 336, 25
 Beaulieu, J.P., Buchler, J.R., Marquette, J.B., Hartman, J.D., Schwarzenberg-Czerny, A. 2006, *ApJ*, 653, L101
 Bonanos, A. Z., Stanek, K. Z., Kudritzki, R. P. et al. 2006, *ApJ*, 652, 313
 Bono, G., Caputo, F., Fiorentino, G., Marconi, M. & Musella, I. 2008, *ApJ*, 684, 102
 Bresolin, F., Kudritzki, R.-P., Méndez, R. H., & Przybilla, N. 2001, *ApJ*, 548, L159
 Bresolin, F., Gieren, W., Kudritzki, R.-P., Pietrzynski, G., & Przybilla, N. 2002, *ApJ*, 567, 277
 Bresolin, F., Pietrzynski, G., Gieren, W., Kudritzki, R. P., Przybilla, N. & Fouque, P. 2004, *ApJ*, 600, 182
 Bresolin, F., Pietrzynski, G., Gieren, W., Kudritzki, R. P. 2005, *ApJ*, 634, 1020
 Bresolin, F., Gieren, W., Kudritzki, R.P., Pietrzynski, G., Urbaneja, M. & Carraro, G. 2009, *ApJ*, 700, 1141
 Bresolin, F., Ryan-Weber, E., Kennicutt R.C. & Goddard, Q. 2009b, *ApJ*, 695, 580
 Deharveng, L., Caplan, J., Lequeux, J., Azzopardi, M., Breysacher, J., Tarenghi, M., Westerlund, B. 1988, *A&AS*, 73, 407
 Evans, C. J. & Howarth, I.D. 2003, *MNRAS*, 345, 1223
 Denicolo, G., Terlevich, R. & Terlevich, E. 2002, *MNRAS*, 330, 69
 Dopita, M.A., Evans, I.N. 1986, *ApJ*, 307, 431
 Fiorentino, G., Caputo, F., Marconi, M. & Musella, I. 2002, *ApJ*, 576, 402
 Freedman et al. 2001, *ApJ*, 553, 47
 Garnett, D.R., Shields, G.A., Skillman, E.D., Sagan, S.P. & Dufour, R.J. 1997, *ApJ*, 489, 63
 Garnett, D. R. 2004, *Element abundances in nearby galaxies*, in Cosmochemistry. The melting pot of the elements. XIII Canary Islands Winter School of Astrophysics, p. 171
 Gieren, W., Pietrzynski, G., Soszynski, I., Bresolin, F., Kudritzki, R. P., Miniti, D., & Storm, J. 2005a, *ApJ*, 628, 695
 Gieren, W. et al. 2005b, *ESO Messenger*, 121, 23
 Gieren, W., Pietrzynski, G., Szewczyk, O., Soszynski, I., Bresolin, F., Kudritzki, Urbaneja, M.A., Storm, J. & Miniti, D. 2008, *ApJ*, 683, 611
 Humphreys, E.M.L., Reid, M.J., Greenhill, L.J., Moran, J.M. & Argon, A.L. 2008, *ApJ*, 672, 800
 Kaufer, A., Venn, K. A., Tolstoy, E., Pinte, C. & Kudritzki, R. P. 2004, *AJ*, 127, 2723
 Kennicutt, R. C., Stetson, P. B., Saha, A. et al. 1998, *ApJ*, 498, 181
 Kewley, L. J. & Ellison, Sara L. 2008, *ApJ*, 681, 1183
 Kewley, L. J. & Dopita, M. A. 2002, *ApJS*, 142, 35
 Kobulnicky, H.A., Kennicutt, R.C. & Pizagno, J.L. 1999, *ApJ*, 514, 544

Komatsu et al., 2009, *ApJS*, 180, 330

Kudritzki, R.-P., Lennon, D. J. & Puls, J. 1995, *Quantitative spectroscopy of luminous blue stars in distant galaxies*, in Proc. ESO Workshop "Science with VLT", Eds. J. P. Welsh & I. J. Danziger

Kudritzki, R.P., 1998, *Quantitative spectroscopy of the brightest blue supergiant stars in galaxies*, in "Stellar Physics for the Local Group", eds. A. Aparicio, A. Herrero & F. Sanchez (Cambridge University Press), p. 149

Kudritzki, R. P. & Puls, J. 2000, *ARA&A*, 38, 613

Kudritzki, R.-P., Bresolin, F., & Przybilla, N. 2003, *ApJ*, 582, L83

Kudritzki, R.-P., Urbaneja, M.A., Bresolin, F., Przybilla, N., Gieren, W. & Pietrzynski, G. 2008, *ApJ*, 681, 269

Kudritzki, R. P. & Urbaneja, M. 2009, *Parameters and Winds of Hot Massive Stars*, STSci Symposium 20, Cambridge University Press, eds. M. Livio & E. Villaver, p126

Lequeux, J., Peimbert, M., Rayo, J. F., Serrano, A. & Torres-Peimbert, S. 1979, *A&A*, 80, 155

Macri, L. M., Stanek, K. Z., Bersier, D., Greenhill, L. J. & Reid, M. J. 2006, *ApJ*, 652, 1133

Mager, V. A., Madore, B. F. & Freedman, W. L. 2008, *ApJ*, 689, 721

Magrini, L., Vilchez, J. M., Mampaso, A., Corradi, R. L. M. & Leisy, P. 2007, *A&A*, 470, 865

Maiolino, R. et al. 2008, *A&A*, 488, 463

Marconi, M., Musella, I. & Fiorentino, G. 2005, *ApJ*, 632, 590

McCarthy, J. K., Lennon, D. J., Venn, K. A., Kudritzki, R. P., Puls, J. & Najarro, F. 1995, *ApJ*, 455, L135

McCarthy, J. K., Kudritzki, R. P., Lennon, D. J., Venn, K. A. & Puls, J. 1997, *ApJ*, 482, 757

McGaugh, S. 1991, *ApJ*, 380, 140

Meynet, & Maeder, A. 2005, *A&A*, 429, 581

Mould, J & Sakai, S. 2008, *ApJ*, 686, L75

Mould, J & Sakai, S. 2009a, *ApJ*, 694, 1331

Mould, J & Sakai, S. 2009b, *ApJ*, 697, 996

Pettini, M. & Pagel, B.E.J. 2004, *MNRAS*, 348, L59

Pietrzynski, G., Thompson, I.B., Graczyk, D., Gieren, W., Udalski, A., Szewczyk, O., Minitti, D., Kolaczkowski, Z., Bresolin, F., Kudritzki, R.P. 2009, *ApJ*, 689, 862

Pilyugin, L.S. 2001, *A&A*, 369, 594

Przybilla, N., Butler, K., Becker, S. R., Kudritzki, R. P. & Venn, K.A. 2000, *A&A*, 359, 1085

Przybilla, N., Butler, K., Becker, S. R., & Kudritzki, R. P. 2001a, *A&A*, 369, 1009

Przybilla, N., Butler, K. & Kudritzki, R. P. 2001b, *A&A*, 379, 936

Przybilla, N. & Butler, K. 2001, *A&A*, 379, 955

Przybilla, N. 2002, thesis, Fakultaet fuer Physik, Ludwig-Maximilian University, Munich

Przybilla, N., Butler, K., Becker, S. R., & Kudritzki, R. P. 2006, *A&A*, 445, 1099

Przybilla, N., Butler, K., & Kudritzki, R. P. 2008a, in "The Metal-Rich Universe", eds. G. Israelian & G. Meynet (Cambridge University Press), in press (astro-ph/0611044)

Przybilla, N., Nieva, M. & Butler, K. 2008b, *ApJ*, 688, L103

Riess, A.G., Macri, L., Li, W. et al. 2009a, *ApJS*, 183, 109

Riess, A.G., Macri, L., Casertano, S. et al. 2009b, *ApJ*, 699, 539

Rizzi, L., Tully, R. B., Makarov, D., Makarova, L., Dolphin, A. E., Sakai, S. & Shaya, E. J. 2007, *ApJ*, 661, 815

Rubin, R.H., Simpson, J.P., Colgan, S.W.J. et al. 2008, *MNRAS*, 387, 45

Saha, A., Sandage, A., Tammann, G.A., Dolphin, A.E., Christensen, J., Panagia, N. & Macchetto, F.D. 2001, *ApJ*, 562, 314

Sakai, S., Ferrarese, L., Kennicutt, R. C., Jr. & Saha, A. 2004, *ApJ*, 608, 42

Sandage, A., Tammann, G.A., Saha, A., Reindl, B., Macchetto, F.D., Panagia, N. 2006, *ApJ*, 653, 843

Schiller, F. & Przybilla, N. 2008, *A&A*, 479, 849

Schlegel, D. J., Finkbeiner, D. P. & Davis, Marc 1998, *ApJ*, 500, 525

Skillman, E. D. 1998, *Chemical Evolution of the ISM in Nearby Galaxies*, in Stellar astrophysics for the Local Group: VIII Canary Islands Winter School of Astrophysics, p. 457

Spergel, D. 2006, *The New Standard Cosmology*, APS April Meeting, April 22-26, 2006, abstract #C5.002

Spergel et al., 2007, *ApJS*, 170, 377

Tegmark, M et al. 2004, *PhysRevD*, 69, 103501

Tremonti, C. A., Heckman, T. M., Kauffmann, G. et al. 2004, *ApJ*, 613, 898

U, V., Urbaneja, M. A., Kudritzki, R.-P., Jacobs, B. A., Bresolin, F. & Przybilla, N. 2009, *ApJ*, 704, 1120

Urbaneja, M. A., Herrero, A., Kudritzki, R.-P., Najarro, F., Smartt, S. J., Puls, J., Lennon, D. J. & Corral, L. J. 2005a, *ApJ*, 635, 311

Urbaneja, M. A., Herrero, A. J., Bresolin, F., Kudritzki, R. P., Gieren, W., Puls, J., J. K., Przybilla, N., Najarro, F. & Pietrzynski, G. 2005b, *ApJ*, 622, 877

Urbaneja, M. A., Kudritzki, R. P., Bresolin, F., Przybilla, N., Gieren, W. & Pietrzynski, G. 2008, *ApJ*, 684, 118

Venn, K. A. 1999, *ApJ*, 518, 405

Venn, K. A., McCarthy, J. K., Lennon, D. J., Przybilla, N., Kudritzki, R. P. & Lemke, M. 2000, *ApJ*, 541, 610

Venn, K. A., Lennon, D. J., Kaufer, A., McCarthy, J. K., Przybilla, N., Kudritzki, R. P., Lemke, M., Skillman, E. D. & Smartt, S. J. 2001, , 547, 765

Venn, K. A., Tolstoy, E., Kaufer, A. et al. 2003, *AJ*, 126, 1326

Vilchez, J.M., Pagel, B.E., Diaz, A.I., Terlevich, E. & Edmunds, M.G. 1988, *MNRAS*, 235, 633

Vlajic, M., Bland-Hawthorn, J. & Freeman, K.C. 2009 *ApJ*, 697, 361

Willner, S.P. & Nelson-Patel, K. 2002, *ApJ*, 568, 679

Zaritski, D., Kennicutt, R. C. & Huchra, J.P. 1994, *ApJ*, 420, 87